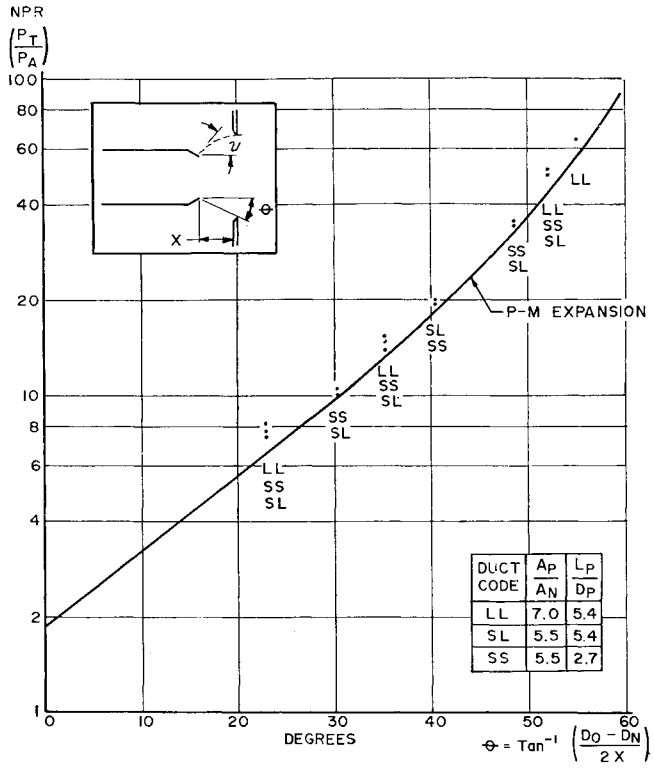


**Fig. 3 Correlation of orifice-installed performance with Prandtl-Meyer expansion at nozzle exit.**

$P_T/P_A$) occurred, after which further increases in SPR produced no effect on NPR. At the vertex of each transition, the NPR was roughly twice the NPR obtained by the duct alone at the same SPR. The SPR and NPR for each transition vertex increased with orifice size, axial position $x$ being constant, until a maximum orifice size that was effective was reached. Increasing orifice size appreciably beyond this critical size resulted in the absence of any orifice effect at all.

Below transition, the jet evidently does not fill the orifice area, and backflow occurs from the duct into the chamber through the orifice. As SPR and hence NPR increase, the jet broadens and approaches the orifice lip until inadequate back-flow can occur to balance the fluid-removal rate from the chamber. At this point, $P_A$ starts dropping rapidly and the jet expands until the lip is contacted. At this point, the original duct backflow is completely sealed off from the chamber and equilibrium is apparently established by a new recirculation pattern from the upstream lip of the orifice, as illustrated in the lower half of Fig. 1b.

The NPR established corresponds to a Prandtl-Meyer expansion at the nozzle throat through an angle $\nu$ approximately equal to the geometric angle $\theta$ defined in Fig. 3. This is demonstrated in Fig. 3 by the comparison between experiment and P-M expansion theory, plotted from Ref. 4, using $\theta$ as the turning angle. Experimental points lie slightly above the P-M line, since the actual turning angle $\nu$ is greater than $\theta$ due to jet curvature.

### Conclusions

1) Backflow is the mechanism by which a steady-state chamber pressure is ultimately established in an ejector-diffuser under conditions of zero secondary flow. Therefore, reduction of backflow into the chamber and removal of backflow from the chamber by a route other than the diffuser duct are possible means of increasing performance. Experimental investigation of a single, simple technique (the inlet orifice plate) indicates that the potential gains are substantial.

2) Backflow is particularly significant for geometries and nozzle pressure ratios characteristic of aircraft engine testing. The basic assumption of normal shock recovery frequently is not satisfied in this case with a straight diffuser duct alone, but can be satisfied by the introduction of an appropriate inlet orifice plate.

3) The nozzle pressure ratio established above transition for a given orifice correlates with a nominal Prandtl-Meyer expansion angle from the nozzle throat to the orifice lip. It follows that axial position $x$, not investigated experimentally, is a governing parameter as well as orifice size.

4) Secondary flow effects, not investigated experimentally by the authors, are of practical interest for turbojet testing, since small secondary flows are generally present because of leakages (e.g., from inlet duct labyrinth seals) and the necessity for engine cooling. However, backflow is still presumably present over some small range of secondary flows, since an arbitrarily small secondary flow could not by itself balance the removal of chamber fluid due to jet-boundary entrainment. Therefore, appropriately sized orifice plates should produce some improvement in ejector-diffuser performance for small secondary-to-primary mass-flow ratios.

### References

[1] Crocco, L., "One-Dimensional Treatment of Steady Gas Dynamics," *Fundamentals of Gas Dynamics, High Speed Aerodynamics and Jet Propulsion*, Vol. 3, Princeton University Press, 1958, p. 291.

[2] Panesci, J. H. and German, R. C., "An Analysis of Second-Throat Diffuser Performance for Zero-Secondary-Flow Ejector Systems," AEDC-TDR-63-249, Dec. 1963, Arnold Engineering Development Center, Tullahoma, Tenn.

[3] Anderson, R. E. and Graham, P. A., "A Study of the Effects of an Orifice Inlet on the Performance of a Straight Cylindrical Diffuser," NAPTC-ATD-143, Dec. 1967, Naval Air Propulsion Test Center, Trenton, N.J.

[4] Ames Research Staff, "Equations, Tables, and Charts for Compressible Flow," Rept. 1135, 1953, NACA.

# Recent Flight-Test Results in Deploying a 20-ft-Diam Ribbon Parachute

William B. Pepper*
*Sandia Laboratory, Albuquerque, N. Mex.*

### Introduction

Sandia Laboratory is conducting a continuing parachute research program to investigate the feasibility of deploying a heavy duty 20-ft-diam ribbon parachute at high dynamic pressures and Mach numbers of 2 to 3. The author[1] earlier reported results of tests up to $M = 2.2$- and 4290- psf dynamic pressure. This paper presents results of data from three additional tests at increased speeds up to $M = 2.43$ and 5700 psf dynamic pressure.

### Apparatus

The specially designed 20-ft-diam ribbon parachute and 19.5-in.-diam test vehicle used on these three tests are described in detail in an earlier paper.[1] The parachute has 30 gores and 30 suspension lines of 12,000-lb tensile strength. Special reinforced selvage ribbons of 2000-, 3000-, and 4000-lb tensile strength are used with only one splice for each horizontal ribbon, the greatest strength being placed in the vent region. Figure 1 shows the 890-lb test vehicle and parachute

Received August 28, 1968. This work was supported by the U.S. Atomic Energy Commission.

* Parachute Project Leader, Rocket and Recovery Systems Division, Aerothermodynamics Projects Department. Associate Fellow AIAA.

**Table 1 20-ft ribbon parachute data summary**[a]

| Test number | Test date | Deployment Conditions: Total (pitot) pressure setting, psia | Pressure switch closure time sec | Altitude, ft mean sea level | Dynamic pressure at switch closure, psf | Mach number | Maximum deceleration, $g$'s | Chute filling time, sec |
|---|---|---|---|---|---|---|---|---|
| 158–11 | 2–15–67 | 65 | 12.6 | 14,111 | 4700 | 2.34 | ND[b] | 0.08 |
| 158–12 | 11–17–67 | 72 | 12.15 | 11,478 | 5100 | 2.29 | 150 | 0.08 |
| 158–13 | 6–12–68 | 80 | 11.39 | 12,000 | 5700 | 2.43 | 200 | 0.07 |

| Test number | Reefing line length, ft | Reefing delay time, sec | Reefed $C_DS$, ft² | Terminal $C_DS$, ft² | Impact velocity, fps | Total time of flight, sec | Total range, ft | Test results |
|---|---|---|---|---|---|---|---|---|
| 158–11 | 12 | 2 | 35 | 133 | 87 | 121.94 | 30,000 | S[c] |
| 158–12 | 12 | 2 | 35 | 130 | 90 | 88.01 | 25,474 | S |
| 158–13 | 12 | 2 | 35 | 130 | 91 | 96.25 | 21,710 | S |

[a] All tests were fired at the Sandia Corporation Tonopah Test Range, Nev., at an elevation of 5338 ft mean sea level using a 30° launch elevation.
[b] ND = No data available.
[c] S indicates successful, no broken suspension lines or canopy ribbons, minor fraying due to ribbon flutter.

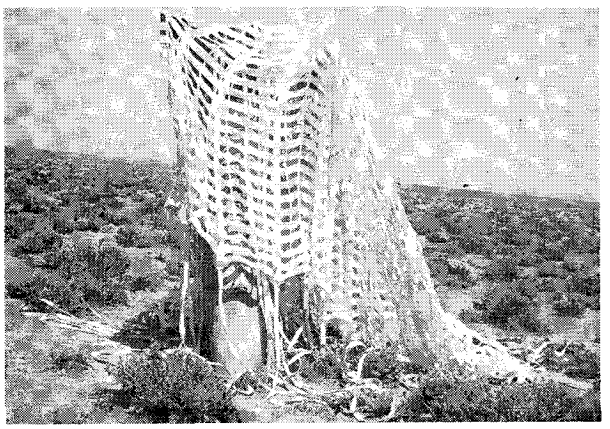

**Fig. 1 20-ft-diam parachute after successful deployment at Mach 2.4.**

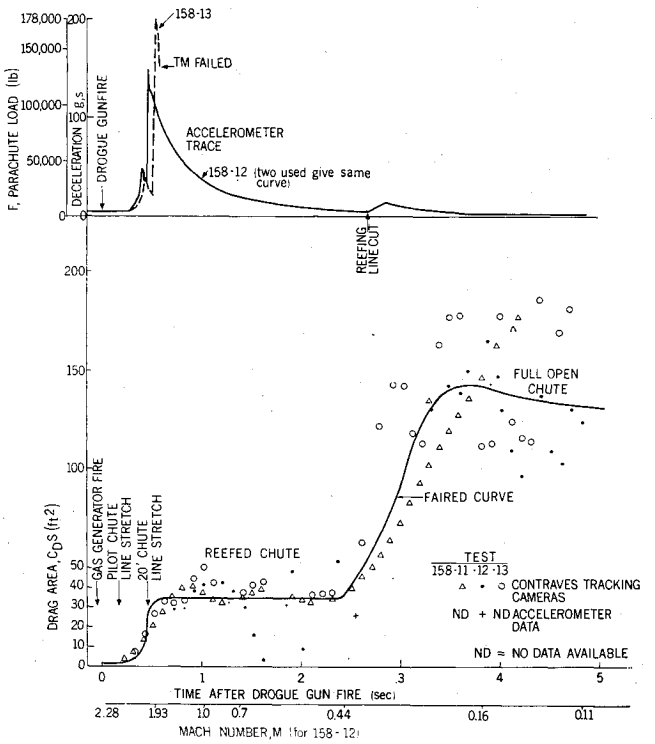


**Fig. 2 Parachute deceleration and drag area variation with time.**

(180 lb packed) after the most recent successful test at $M$ = 2.43. Two Nike rockets fired in series are used to boost the vehicle from a 30° elevation ground launching at the Tonopah Test Range, Nev., to maximum conditions at burnout of the second stage which are approximately $M$ = 3 and a dynamic pressure of 9000 psf. A total head (pitot) pressure switch is used to fire the drogue gun and deploy the 18-in. pilot parachute at the desired dynamic pressure after coast. An eight-channel telemetering system in the vehicle is used to measure deceleration of the unit after parachute deployment.

### Results

Data obtained from the three successful tests at 4700-, 5100-, and 5700-psf dynamic pressure are listed in Table 1. The maximum opening load shown in Fig. 2 recorded by the on-board telemetry system using accelerometers was 200 $g$'s or 178,000 lb at a Mach number of 2.43. The first-stage filling times were less than 0.1 sec. The terminal descent drag area was approximately 130 ft², which is equivalent to a drag coefficient of 0.415 for this relatively porous parachute. The reefed drag area, shown in Fig. 2, for the 2-sec reefing period was approximately 35 ft², which is plotted relative to other data[2] in Fig. 3. The reefed drag area shown in the lower portion of Fig. 2 is constant over the Mach number

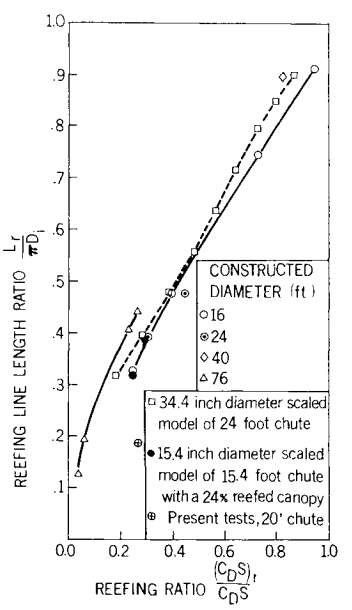


**Fig. 3 Variation of reefing ratio with reefing line length ratio for ribbon parachutes.**

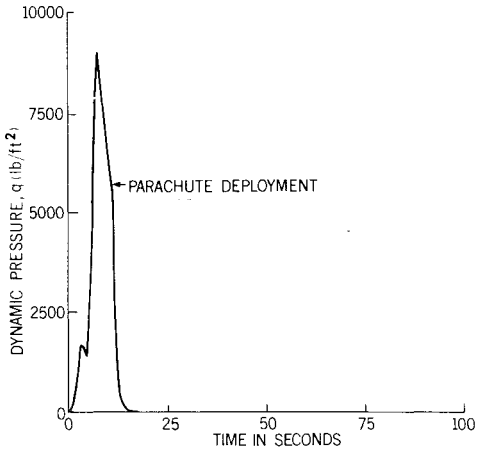


**Fig. 4 Variation of dynamic pressure with time for test 158-13.**

range of 1.92 to 0.44 and values obtained from the upper deceleration curve by using $C_DS = F/q$ agree fairly well with the contraves tracking camera trajectory data.

The decay in dynamic pressure with time from launch for test 158–13 is shown in Fig. 4. The sharp trajectory alteration at parachute deployment is graphically illustrated in Fig. 5 as obtained from the Contraves Cinetheodolites.[3]

Two coats of RTV silicone rubber cement were applied to the guide surface pilot chute and the suspension lines of the 20-ft chute on all three tests to act as an ablator for the aerodynamic heating resulting from the approximate 500°F stagnation temperature.

### Conclusions

A series of three Nike/Nike rocket-boosted tests of a specially designed 20-ft-diam ribbon parachute has been conducted. It is concluded that 1) the chute is suitable for use up to $M = 2.43$ and a dynamic pressure of 5700 psf using a 1100-lb total weight test vehicle system and 2) both the 18-in.-diam pilot chute and reefed main 20-ft chute operated in a stable configuration and without damage during deployment.

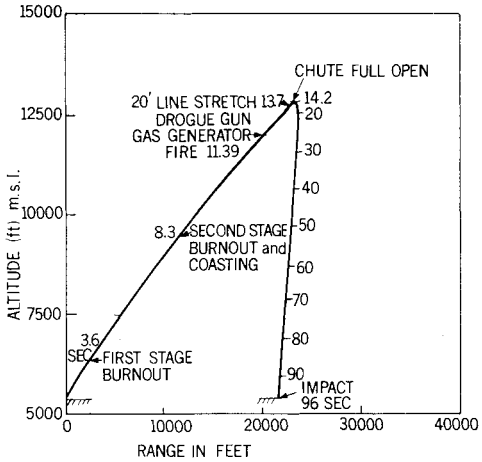


**Fig. 5 Variation of altitude with range for test 158-13.**

### References

[1] Pepper, W. B., "A 20-ft-Diameter Ribbon Parachute for Deployment at Dynamic Pressures above 4000 psf," *Journal of Aircraft*, Vol. 4, No. 3, May-June 1967, pp. 265–267.

[2] Cordell, T. L., "Ordinary Reefed Parachutes as Mach-4 Decelerators," TM-65-520, Nov. 1965, Sandia Corp.

[3] "Summary Sandia Corporation Field Test Facilities," SM FTACS-O, April 1967, Sandia Corp.

# A New Solution for the Skin-Friction Drag on a Cylinder

E. P. Russo*
*Louisiana State University, New Orleans, La.*
AND
O. A. Arnas†
*Louisiana State University, Baton Rouge, La.*

### Introduction

THE generally accepted formulation for the skin-friction drag on a right circular cylinder is due to Thom.[1,2] He calculated the skin friction up to 60° from the forward stagnation point by using a closed-form approximate solution of the boundary-layer equations, and by taking values between 60° and 90° from experiment, thus deducing $3.84(Re)^{-1/2}$ as the skin-friction drag coefficient for the front half of the cylinder. With a small addition for the contribution of the rear half, Thom gave $4.0(Re)^{-1/2}$ as a close estimate of this coefficient. The analysis given in this paper is formulated on the basis of Blasius' solution for flow past a right circular cylinder. The integration is carried out from the stagnation point to the point of separation. The results of the integration can be arranged as a sum of easily computed terms, which heretofore have gone unnoticed.

### Analysis

The Blasius velocity distribution[3] for the flow around a right circular cylinder of radius $R$ is

$$u = 2U_\infty \left\{ \left(\frac{x}{R}\right) f_1'(\eta) - \frac{4}{3!}\left(\frac{x}{R}\right)^3 f_3'(\eta) + \frac{6}{5!}\left(\frac{x}{R}\right)^5 f_5'(\eta) - \ldots \right\} \quad (1)$$

where $x$ denotes the distance from the stagnation point measured along the contour of the cylinder, $U_\infty$ is the free-stream velocity and

$$\eta = y(Re)^{1/2}/R \quad (2)$$

where the Reynolds number $Re$ is equal to $2U_\infty R/\nu$, and $y$ is measured perpendicular to the cylinder surface. The function $f'(\eta)$ is tabulated elsewhere.[4]

The viscous drag per unit length on the cylinder may be calculated by evaluating the following integral which is the defining equation for the skin-friction drag:

$$D_F = 2\int_0^\beta \mu \left.\frac{\partial u}{\partial y}\right|_{y=0} \cos\Phi dx \quad (3)$$

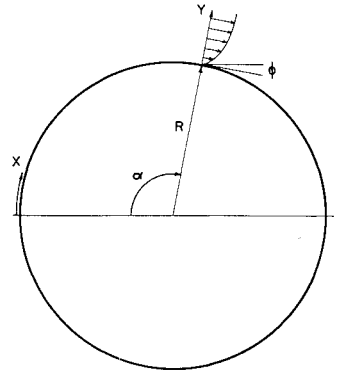


**Fig. 1 Cylinder cross section showing coordinate references and angles.**

Received August 13, 1968.

* Assistant Professor of Engineering. Member AIAA.
† Associate Professor, Mechanical Engineering Department. Member AIAA.